

See discussions, stats, and author profiles for this publication at: <https://www.researchgate.net/publication/220050290>

# Image splitting techniques for a dual layer high dynamic range LCD display – art. no. 6917oM


Article in Journal of Electronic Imaging · October 2008

DOI: 10.1117/12.769692 · Source: DBLP

CITATIONS  
16

READS  
1,368

3 authors:




Gabriele Guarnieri

Amped Software

15 PUBLICATIONS 146 CITATIONS

SEE PROFILE




Luigi Albani

BARCO NV

40 PUBLICATIONS 172 CITATIONS

SEE PROFILE



Giovanni (Gianni) Ramponi

University of Trieste

199 PUBLICATIONS 4,389 CITATIONS

SEE PROFILE

Some of the authors of this publication are also working on these related projects:

- Project

Tone mapping [View project](#)
- Project

Visual Privacy [View project](#)

# Image-splitting techniques for a dual-layer high dynamic range LCD display

**Gabriele Guarnieri**

University of Trieste  
Dipartimento di Elettrotecnica, Elettronica e Informatica  
Via Valerio 10  
34127 Trieste, Italy  
E-mail: gguarnieri@units.it

**Luigi Albani**

FIMI-Philips  
Via Saul Banfi 1  
21047 Saronno (VA), Italy

**Giovanni Ramponi**

University of Trieste  
Dipartimento di Elettrotecnica, Elettronica e Informatica  
Via Valerio 10  
34127 Trieste, Italy

**Abstract.** Liquid crystal displays (LCDs) are replacing analog film in radiology and reducing diagnosis times. Their typical dynamic range, however, can be too low for some applications, and their poor ability to reproduce low-luminance areas represents a critical drawback. The black level of an LCD can be drastically improved by stacking two liquid crystal panels in series. In this way the global transmittance is the pointwise product of the transmittances of the two panels and the theoretical dynamic range is squared. Such a high dynamic range (HDR) display also permits the reproduction of a larger number of gray levels, increasing the bit depth of the device. The two panels, however, are placed at a small distance from each other due to mechanical constraints, and this introduces a parallax error when the display is observed off-axis. A complex, spatially adaptive algorithm is therefore necessary to generate the images used to drive the two panels. We describe the characteristics of a prototype dual-layer HDR display and discuss the issues involved in the image-splitting algorithms. We propose some solutions and analyze their performance, giving a measure of the capabilities and limitations of the device. © 2008 SPIE and IS&T. [DOI: 10.1117/1.3010884]

## 1 Introduction

Consumer displays sold today are almost totally of the liquid crystal display (LCD) type. They offer a flat surface and small physical dimensions, a high brightness and resolution, no flicker, no geometric distortion, good longevity, low power consumption, and low electromagnetic emissions. LCDs are also widespread in medical imaging appli-

cations and are gradually replacing analog film in radiology. However, LCDs still do not match the performance of traditional radiographic film. A film-based X-ray viewed on the traditional light box can reach a peak brightness of around 4000 cd/m<sup>2</sup> and a dynamic range (defined as peak brightness divided by black level) of around 3000:1, whereas an LCD display can reach a few hundred cd/m<sup>2</sup> and a dynamic range below 3 orders of magnitude. In particular, LCD displays have a poor dark-level performance, because the panel is not able to completely block the light coming from the backlight unit. This may be unacceptable in some medical applications where a high dynamic range is necessary in order to discriminate a larger number of luminance levels and detect fine details with very small luminance differences.

The black level of an LCD monitor can be drastically reduced by stacking two panels in series<sup>1</sup> or by using spatially modulated backlights.<sup>2–4</sup> In the former case, the global transmittance is the pointwise product of the transmittances of the two panels and the theoretical dynamic range is squared. The grayscale reproduction accuracy is also increased, because the light coming from the backlight unit is modulated twice, although the resulting bit depth is not doubled because different combinations of the two panels can produce the same output level. Unlike a conventional display, a dual-layer display cannot be directly connected to the output of a PC graphics card or a compatible image source; some processing is necessary in order to generate the two images which drive the two panels. For this purpose, one major difficulty comes from the fact that the two panels are placed at a small distance from one another due to mechanical constraints, and therefore some parallax error

Paper 07235R received Dec. 17, 2007; revised manuscript received Jul. 24, 2008; accepted for publication Aug. 31, 2008; published online Nov. 6, 2008. This paper is a revision of a paper presented at the SPIE conference Medical Imaging 2008: Image Perception, Observer Performance, and Technology Assessment, February 2008, San Diego, California. The paper presented there appears (unrefereed) in SPIE Proceedings Vol. 6917.

is introduced if the position of the user is not orthogonal to the panel. The error can be reduced by means of appropriate image-processing techniques.

Alternative designs exist for high dynamic range (HDR) displays, which use a single LCD panel combined with a spatially varying backlight unit, typically consisting of an array of individually modulated LEDs which are dimmed locally in correspondence to the dark areas of the image.<sup>2,3</sup> This solution also requires the use of complex image-processing techniques, because the LED array has a significantly lower resolution than the LCD panel, and is critical with regard to the high power consumption and consequent thermal problems.

In this paper, we discuss the issues involved in the image-splitting algorithms for a prototype HDR display based on dual-layer LCD technology. We propose some solutions to the problem and analyze their performance. The results allow to give a measure of the capabilities and of the physical limitations of the device. This paper is structured as follows. In Section 2 we describe the hardware characteristics of the prototypes and their operating principles. In Section 3, we introduce an expression for the parallax error which is intrinsically present in a dual-layer display, in order to prove the need for a dedicated image-splitting algorithm; we then illustrate the general issues and requirements involved in such techniques. In Sections 4 and 5 we propose two image-splitting techniques, which guarantee a perfect reconstruction of the image when the two panels are aligned, and try to minimize the parallax error introduced by off-axis view. The first proposed method is a simple improvement on a heuristic technique and is closely related to a well-known image-processing problem. This similarity allows the use of some prior art techniques which are available in the literature, although applied to different problems. However, this method still has some limitations which suggest the design of a new operator. The second proposed method seeks an optimal solution to the splitting problem by performing a constrained minimization of an appropriate functional. In Section 6 we discuss the results obtained using the second proposed method and some open issues. Because the method is based on a constrained optimization procedure, in which the objective function measures the parallax error and the constraints are strictly derived from the device specifications, the results give a measure of the capabilities and physical limitations of the proposed dual-layer display. Finally, in Section 7 we conclude and give an overview of the future work.

## 2 Dual-Layer LCD Prototypes

Several prototypes of dual-layer LCD displays for medical imaging applications were built at FIMI-Philips and are currently under testing. Each prototype was built using two grayscale IDTech 18 in. LCD panels. After removing the original backlight unit, the individual LCD glass panels were mechanically matched one on top of the other, taking care to align the active areas at best, and finally combined to a single high-brightness backlight unit. The panel facing the backlight unit is referred to as the “backpanel,” and the one seen by the viewer is referred to as the “frontpanel.” The driving electronics is properly arranged in order to allow each panel to be driven independently from a standard

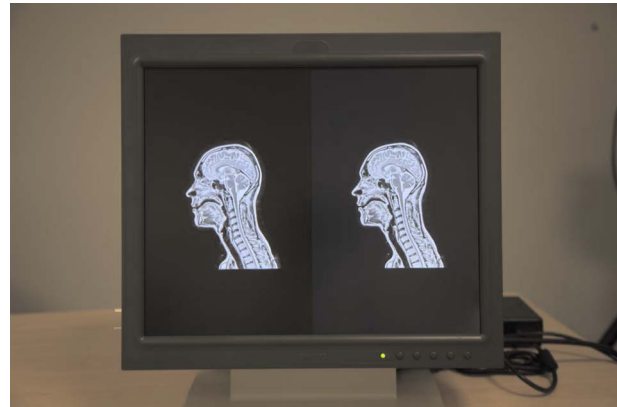


Fig. 1 Prototype of dual-layer LCD display.

digital visual interface (DVI) input. To operate the display, a standard PC is used on which a graphics card with dual DVI output is installed. Each panel of the dual-layer monitor is attached to one output. A specific software package has been developed for the proper generation of the two images which drive the frontpanel and the backpanel of the prototype.

A picture of a prototype is visible in Fig. 1. On the left half of the screen, the dual-layer display is fully exploited. For comparison, on the right half of the screen a conventional single-layer LCD is simulated by displaying the whole image on the frontpanel and a white background on the backpanel. The improved black level of the dual-layer display is clearly visible. Besides the high dynamic range and the improved bit depth, the grayscale dual-layer LCD prototype also features enhanced performance in terms of viewing angle, in the sense that a reduced luminance drop-off with angle compared to a conventional display was measured. The current prototype is calibrated for a maximum luminance of 500 cd/m<sup>2</sup> and, when measured in a dark environment, can reach a black level below 0.01 cd/m<sup>2</sup>, corresponding to a dynamic range of over 50,000.

Color prototypes have also been built by stacking a color frontpanel over a grayscale backpanel. Color LCD panels, however, have a lower transmittance than the grayscale ones due to the presence of the color filters; this creates the need for a higher-brightness backlight unit, which can be critical with regard to heat dissipation. We did not consider the use of a color backpanel, because it would further reduce the peak brightness and likely introduce moiré artifacts without introducing a significant benefit. Besides having a lower peak brightness, color prototypes also have less importance in the current medical applications, because a high dynamic range is typically required in radiology, which mostly involves the display of grayscale data.

## 3 Splitting Algorithms

The processing used to generate the two images to be displayed on the two panels plays a fundamental role in the performance of the device. The simplest possible technique is to perform the splitting on a pixel-by-pixel basis. More precisely, if we indicate with  $L_{in}(x,y)$  the luminance of the input image at pixel location  $(x,y)$  and with  $L_b(x,y)$  and

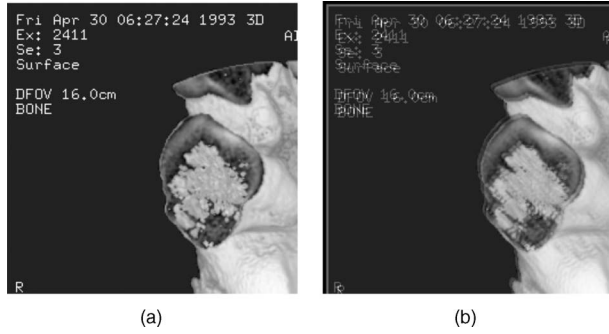


**Fig. 2** Example of parallax error with square-root splitting: (a) original image and (b) simulation of the displayed image with a horizontal and vertical shift of 3 pixels in the backpanel.

$L_f(x,y)$  the luminance of the backpanel and frontpanel, respectively, the splitting algorithm takes the form

$$L_b(x,y) = F[L_{in}(x,y)] \quad L_f(x,y) = \frac{L_{in}(x,y)}{L_b(x,y)}. \quad (1)$$

In other words, the backpanel is computed by mapping the input luminance with a suitable nonlinear function  $F(\cdot)$ , and the frontpanel is subsequently computed by division in order to guarantee that the product of the two images reproduces the input. The luminance values in Eq. (1) and the following are expressed in normalized units; this allows us to simplify the notation by dropping any scaling factors and to consider without distinction the output luminance or the panel transmittance. The splitting is computed on linear data; the nonlinear encoding of the source image (if present) and the response of the liquid crystal panels are compensated appropriately by mapping the data before and after the processing. An intuitive choice for the function  $F(\cdot)$ , suggested by the symmetry of the system, is a square root;<sup>5</sup> in this way, each panel displays the same image. However, in a real device the liquid crystals are enclosed between two glass plates which introduce a finite distance between the planes on which the images are formed, even if the two panels are in contact. Instead of seeing the correct image  $L_{out}(x,y) \triangleq L_b(x,y)L_f(x,y)$ , as observer looking at the display from an off-axis position sees a distorted image  $\tilde{L}_{out}(x,y) \triangleq L_b(x+\Delta x, y+\Delta y)L_f(x,y)$ , where the displacements  $\Delta x$  and  $\Delta y$  depend on his viewing angle. This form of distortion is referred to as parallax error and gives rise to artifacts such as those shown in Fig. 2. The IDTech panels used in the prototypes are approximately 1.6 mm thick and have an active area of  $359.0 \times 287.2$  mm. For instance, a viewer at a distance of 70 cm and aligned to one corner of the display sees the backpanel at the opposite corner shifted by  $\Delta x = 0.8$  mm horizontally and  $\Delta y = 0.7$  mm vertically.

It is convenient to measure the distortion in the perceived image with the relative error:

$$E(x,y) \triangleq \frac{L_b(x+\Delta x, y+\Delta y)L_f(x,y) - L_b(x,y)L_f(x,y)}{L_b(x,y)L_f(x,y)} = \frac{L_b(x+\Delta x, y+\Delta y) - L_b(x,y)}{L_b(x,y)}. \quad (2)$$

With this choice, an expression is derived which depends on the backpanel only. The use of the relative error also has a perceptual motivation, because the perception of luminance by the human visual system approximately follows Weber's law. Weber's law only holds in a limited range of luminance levels; however, a more accurate measure would yield an expression which also depends on the frontpanel and would greatly increase the problem complexity.

In order to reduce the distortion, the backpanel image should be blurred, so that a small displacement does not alter the pixel values excessively. The frontpanel image is then sharpened to compensate for the blurring. Designing the corresponding algorithm is a nontrivial task which should meet different and conflicting requirements:

1. Feasibility: The transmittances computed by the splitting algorithm should be greater than the panel black level and smaller than the panel white level.
2. Perfect reconstruction: The image resulting from the combination of the backpanel and the frontpanel should be equal to the input image when the two panels are aligned. In any case, the splitting algorithm should be designed in order to minimize the visibility of the reconstruction error.
3. Parallax error reduction: The splitting algorithm should exploit the available degrees of freedom in order to minimize the reconstruction error when the two panels are viewed from a misaligned direction.
4. Computational efficiency: The computational complexity of the splitting algorithm should be low enough to allow real-time processing on a standard PC or on low-cost graphics hardware.

In this paper we consider a first class of splitting algorithms which meet the perfect reconstruction constraint:

$$L_b(x,y)L_f(x,y) = L_{in}(x,y) \quad \forall (x,y). \quad (3)$$

This simplifies the problem, because only the backpanel needs to be computed; the frontpanel is then generated automatically by division. It is also possible to compute the frontpanel first, but the former approach is more natural to follow because the design objectives are easier to express for the backpanel. After splitting, the frontpanel and backpanel luminances are converted to digital driving levels and quantized to 8 bits. As previously noticed, a nonlinear mapping must be performed in order to compensate for the distortion introduced by the panels; this operation is commonly known as gamma correction. For greater accuracy, we measured the actual response of the panels used in the prototypes, rather than using an analytical curve defined in standard recommendations for display or television devices.<sup>6</sup> The pixels of grayscale LCD panels are actually made of three subpixels which can be independently driven by the three RGB channels of the DVI input. This permits the use of subpixel dithering in order to improve the perceived bit depth of the device.



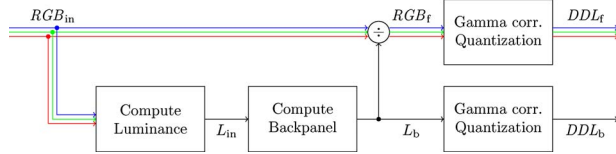


**Fig. 3** Block diagram of a perfect-reconstruction splitting algorithm.

A splitting algorithm can be extended to color images with only minor modifications. The splitting is computed on the luminance only, because a grayscale backpanel must be generated in any case; the frontpanel is then computed by dividing each of the RGB channels of the input image by the backpanel. It is convenient to compute the luminance by taking the maximum of the three RGB channels, following the definition used in the hue-saturation-value (HSV) color space. With this choice, the three channels of the frontpanel image are upper bounded by the corresponding grayscale image, and it is easier to prevent unwanted clipping.

A block diagram of a generic perfect-reconstruction algorithm is shown in Fig. 3. The critical part in the algorithm is clearly the computation of the backpanel, and in the following we describe some possible solutions.

#### 4 Method 1: Constrained Filtering of the Backpanel

A simple improvement on the square-root technique described in the previous section consists of blurring the square root of the input image with a lowpass filter in order to obtain a smooth backpanel. The frontpanel is then computed by division, following the scheme of Fig. 3:

$$L_b(x, y) = \text{BLUR}[\sqrt{L_{in}(x, y)}] \quad L_f(x, y) = \frac{L_{in}(x, y)}{L_b(x, y)} \quad (4)$$

Blurring is a nontrivial task, because it must take into account the limited dynamic range of the panels. If a linear lowpass filter is used, a portion of the pixels in the backpanel are darker than  $\sqrt{L_{in}}$ , and the corresponding pixels in the frontpanel are brighter; if no precaution is taken, some pixels in the frontpanel might exceed the white level. An example of this problem on a 1-D test signal is shown in Fig. 4. In order to prevent the clipping of the frontpanel, some sort of nonlinear filter must be used.

A problem which often arises in signal and image processing is the computation of constrained lowpass filters, or envelopes. This operation basically consists of approximating a signal with a smoother function, which is bounded from below by the signal itself. The effect can be visually interpreted as an elastic rope or membrane resting on top of

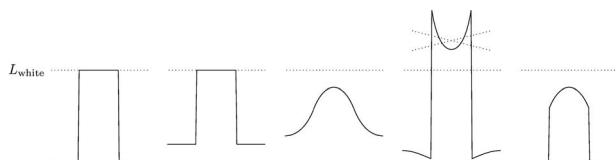


**Fig. 4** Saturation artifacts: (left to right) input signal, square root, backpanel, frontpanel with clipping, and reconstructed signal.

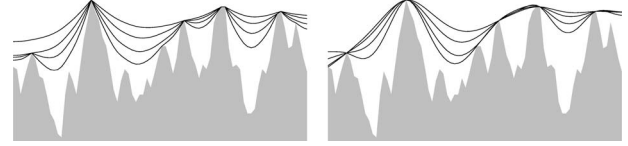


**Fig. 5** Membrane-based and spline-based envelope filters with different bandwidths.

the signal graph. If a higher smoothness is required, it is possible to simulate the behavior of an elastic beam or plate, typically by means of spline models. A comparison of the two formulations on a 1-D signal is illustrated in Fig. 5; the main difference is that a membrane-based envelope can have a discontinuous first derivative in the points where the constraint is active, whereas spline-based envelopes are smooth in this case.

A possible technique which avoids the clipping of the frontpanel consists of filtering the square root of the input image with a constrained low-pass filter rather than a simple linear lowpass filter. The backpanel computed in this way meets by definition the constraint  $L_b(x, y) \geq \sqrt{L_{in}(x, y)}$ . Consequently, the frontpanel computed by division is upper bounded by the square root, which is lower than the white level, provided that the input image is suitably scaled, and clipping is avoided:

$$L_b(x, y) \geq \sqrt{L_{in}(x, y)} \Rightarrow L_f(x, y) = \frac{L_{in}(x, y)}{L_b(x, y)} \leq \sqrt{L_{in}(x, y)} \quad (5)$$

This property is visualized in Fig. 6 using a simple 1-D test signal. An application to a real image is shown in Fig. 7.

A constrained lowpass filter can be implemented in several ways. A heuristic approach may consist of blurring the image with a linear lowpass filter and then adding an offset to the output or parts of it. More advanced methods may formulate the filtering operation as a constrained optimization problem. A possible objective function is

$$\iint \{|\nabla f(x, y)|^2 + \lambda [f(x, y) - u(x, y)]^2\} dx dy = \min$$

subject to  $f(x, y) \geq u(x, y)$ , (6)

where  $u(x, y)$  is the input image,  $f(x, y)$  is the filtered output, and the integral is computed over the whole image area. The first term privileges a smooth output, and the second term privileges an output which closely approximates the input; the scalar  $\lambda$  allows to set the tradeoff between these two objectives and adjust the “bandwidth” of the filter. A spline-based filter can be obtained by replacing the first term in Eq. (6) with a thin plate spline energy functional; this approach involves higher-order derivatives

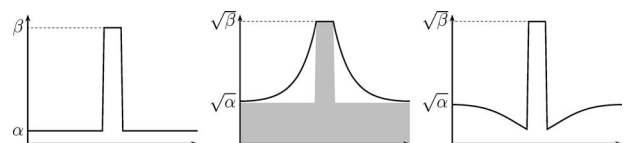


**Fig. 6** Example of splitting for a 1-D test signal: (Left to right) input, backpanel, and frontpanel.

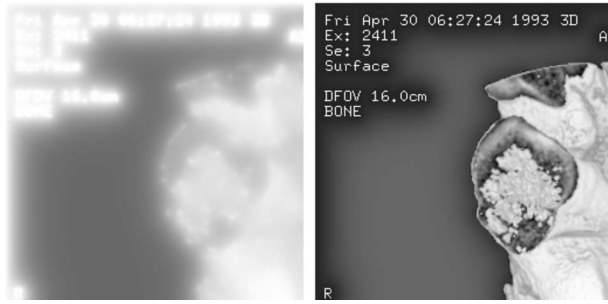


**Fig. 7** Backpanel and frontpanel computed with square root and constrained lowpass filter.

and has a remarkably higher computational complexity. Once Eq. (6) is discretized, a quadratic programming problem is obtained, which can be solved by means of appropriate iterative methods that exploit its structure and sparsity.

The computation of constrained lowpass filters typically arises in a class of algorithms for the dynamic range reduction of images based on the Retinex model of the human visual system (HVS).<sup>7,8</sup> According to the model, the luminance in an image is given by the pointwise product of the illumination which depends on the light sources, and the reflectance, which instead depends on the objects. Studies on the HVS have revealed that the visual sensation mostly depends on the object reflectance and remains unaltered if the light source illuminating the scene is changed within certain limits. Retinex-based algorithms attempt to decompose the input image into the product of illumination and reflectance; the illumination is then mapped in order to reduce its dynamic range, while the reflectance is left unaltered or optionally enhanced. The illumination is typically a smooth function and is always larger than the image luminance, because the objects reflect only a fraction of the incident light; based on these assumptions, a constrained lowpass filter appears a suitable operator for the estimation of this component. The problem of illumination estimation in Retinex-based algorithms bears some remarkable similarities to the image splitting in a dual-layer display; therefore, we made some attempts to adapt techniques developed for the former problem to the present application. One interesting technique was introduced by Frankle and McCann.<sup>9</sup> In this method, a narrowband lowpass filter is computed efficiently using a cascade of convolutions with large but very sparse kernels; the constraint is incorporated by means of a threshold operation after each convolution. A multiresolution implementation which further reduces the computational cost was later introduced.<sup>10</sup> Recursive filters have also been investigated,<sup>11</sup> but the presence of the constraint can give rise to banding artifacts in the filtered image. Variational methods have been recently proposed.<sup>12,13</sup> Despite the similar objective, algorithms designed for Retinex applications often have some quality issues which make them inapplicable for the computation of the backpanel in a dual-layer display. This happens because, in the former application, artifacts introduced by the constrained lowpass filter generally produce a hardly noticeable error in the output image; therefore, the quality requirements are much lower than in the present case. In particular, many



**Fig. 8** Example of parallax error with synthetic images.

algorithms are unable to completely smooth out sharp edges. However, the illumination component in an image can contain sharp edges in the points where an object covers the light source; therefore, the preservation of edges is a desired feature rather than an artifact, and indeed some formulations of the Retinex algorithm use edge-preserving lowpass filters which take this property into account and avoid the formation of unwanted halos.

The images shown in this paper were generated using the quadratic programming formulation.<sup>6</sup> We used a modified conjugate gradient method to solve the constrained optimization problem, because its behavior is well known theoretically. Good results were also obtained using the Frankle–McCann algorithm. An efficient implementation is currently under study, and one possible option may involve the use of multigrid methods,<sup>14,15</sup> which are among the fastest known algorithms for the solution of the linear systems obtained from the discretization of partial-differential equations or variational problems. The basic idea of multigrid methods is to generate an approximate solution by down-sampling the input image (typically by a factor of 2), filtering it, and up-sampling the result back to the original size. This approximate solution is used as a starting guess for an iterative method such as Gauss–Seidel or Jacobi. The method is applied recursively on the downsampled image until the corresponding linear system is small enough to allow a direct solution, for instance by means of the familiar Gaussian elimination.

## 5 Method 2: Generation of the Backpanel Image by Constrained Optimization

In the algorithm described above, the constraints have an asymmetric nature, because they only include a lower bound for the backpanel. In presence of dark details on a light background, the constrained lowpass filter tends to “fill the hole,” producing a uniform backpanel, and the detail is reproduced on the frontpanel only. In the case of light details on a dark background, the backpanel must follow the transition as shown previously in Fig. 6, and on some critical images this variation in the backpanel can give rise to visible parallax error even if a narrowband lowpass filter is used. Artifacts can appear especially around synthetic parts of the image such as text or frames over a uniform dark background. An example is shown in Fig. 8. Improved

implementations of the constrained lowpass filter can reduce this problem but not avoid it completely, because it is intrinsically present in the method.

Moreover, the constraints themselves can be chosen in a more clever way. By using a constrained lowpass filter, the backpanel and the frontpanel are bounded, from below and from above, respectively, by the square root of the input image as shown in Eq. (5). These constraints can be relaxed in order to exploit some further degrees of freedom without compromising the feasibility of the solution.

Finally, by using a constrained lowpass filter to blur the backpanel, it is guaranteed that the frontpanel image does not exceed the white level. An examination of Fig. 6, however, shows that the frontpanel computed in this way presents some undershoots near sharp edges; in some cases, these pixels may fall below the black level, and dark details are lost. In order to prevent this artifact, some sort of double constraint must be used.

In order to derive the exact constraints, we shall suppose that each pixel of the two panels can have a normalized transmittance between  $1/d$  and 1, where  $d$  is the dynamic range. The maximum transmittance of an LCD panel is actually much lower (0.33 for the IDTech grayscale panels used in the prototypes, 0.1 for color panels), but we use normalized units for simplicity of notation. By definition, the backpanel does not saturate if the displayed image  $L_b(x, y)$  is within the limits:

$$\frac{1}{d} \leq L_b(x, y) \leq 1 \quad \forall (x, y) \quad (7)$$

If perfect reconstruction is requested, the frontpanel is computed by division. The constraints in this case are

$$\begin{aligned} \frac{1}{d} &\leq \frac{L_{in}(x, y)}{L_b(x, y)} \leq 1 \\ \Rightarrow L_{in}(x, y) &\leq L_b(x, y) \leq dL_{in}(x, y) \quad \forall (x, y) \end{aligned} \quad (8)$$

Therefore, merging the two sets of constraints in Eq. (7) and (8), we obtain that both panels do not saturate if the backpanel satisfies

$$\max\{L_{in}(x, y), 1/d\} \leq L_b(x, y) \leq \min\{dL_{in}(x, y), 1\} \quad \forall (x, y) \quad (9)$$

If the dynamic range of the input image is greater than  $d^2$ , the constraints in Eq. (9) become incompatible; therefore, the input image should be preprocessed in order to remove any exceedingly dark pixels. This is unnecessary if the digital data of the source image are decoded following a DICOM<sup>16</sup> grayscale display function which matches the dynamic range of the display device.

Based on the assumption that the parallax error is small if the backpanel image is smooth, the proposed method generates, by means of an optimization procedure, the smoothest possible backpanel image subject to the constraints in Eq. (9). Smoothness can be measured in several ways, and the measure we propose is suggested by the expression of the relative error in Eq. (2). Because the backpanel we are seeking is a smooth function and the displacements  $\Delta x$  and  $\Delta y$  are small, we approximate Eq. (2) with a first-order Taylor expansion:

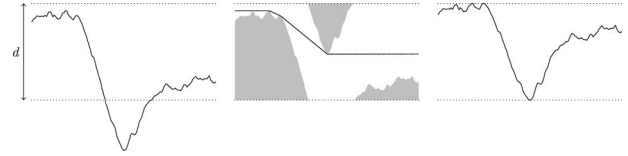


**Fig. 9** Second proposed method applied to a 1D test signal: (left to right) input signal, backpanel and constraints (shaded), and frontpanel. The vertical axis is in logarithmic scale for a better legibility.

$$\begin{aligned} E(x, y) &\triangleq \frac{L_b(x + \Delta x, y + \Delta y) - L_b(x, y)}{L_b(x, y)} \\ &\approx \frac{1}{L_b(x, y)} \left[ \frac{\partial L_b(x, y)}{\partial x} \Delta x + \frac{\partial L_b(x, y)}{\partial y} \Delta y \right] \\ &= \frac{\nabla L_b(x, y)}{L_b(x, y)} \cdot \begin{bmatrix} \Delta x \\ \Delta y \end{bmatrix}. \end{aligned} \quad (10)$$

where  $\cdot$  indicates a scalar product. In order to obtain a single scalar which can be minimized by an optimization procedure, we compute the mean-square norm of the gradient term in the right side of Eq. (10), thus obtaining the following expression in which the identity follows from simple calculus:

$$E_{\text{mean}} \triangleq \iint \left| \frac{\nabla L_b(x, y)}{L_b(x, y)} \right|^2 dx dy = \iint |\nabla \log L_b(x, y)|^2 dx dy. \quad (11)$$

This approach is different from the one described in Section 4. The backpanel is not computed by means of some sort of lowpass filter, applied to an appropriate signal such as the square root of the input image; it is instead generated by an optimization procedure, and its shape is only determined by the constraints. The proposed method theoretically produces an optimal result, because the objective function in Eq. (11) measures the parallax error and the constraints in Eq. (9) are strictly derived from the device specifications. The method is also easy to use, because it does not contain any free parameter which requires a manual adjustment. An example of its behavior on a 1-D test signal is shown in Fig. 9. The algorithm produces a constant backpanel wherever possible; if the dynamic range of the input signal is less than  $d$ , the signal is displayed on the frontpanel only and the parallax error is completely avoided. In the bright areas, the lower bound is active and the backpanel takes the value  $L_b(x, y) \geq L_{in}(x, y)$ ; in the dark areas, the upper bound is active and the backpanel takes the value  $L_b(x, y) \leq dL_{in}(x, y)$ . The step in the backpanel is therefore approximately  $d$  times smaller than the step in the input signal; it can also be noticed that the lower bound in Eq. (9) is lower than the square root of the input image, so there is a better chance that the algorithm produces a smooth backpanel. If no constraint is active, the backpanel forms a linear slope (in logarithmic scale) in order to minimize the functional in Eq. (11).

On 2-D images, the algorithm performs in a similar way. The backpanel computed with the proposed method is similar to a membrane-based envelope, with the difference being that the membrane is not attracted to an input signal



[mathematically, this means setting  $\lambda=0$  in Eq. (6)] and its shape is only determined by the constraints. In the areas where no constraint is active, the backpanel satisfies the Laplace equation. The use of higher-order smoothness functionals, such as a thin-plate-spline bending energy, was not considered both for computational efficiency and for a theoretical motivation. The membrane smoothness functional minimizes the average slope of the backpanel and therefore produces a constant output when possible; the spline functional instead minimizes the bending energy and does not penalize a steep gradient.

Performing a constrained optimization with a large number of unknowns might seem a computationally complex task. On the contrary, the proposed method can be implemented very efficiently by means of multigrid techniques.<sup>14,15</sup> An unoptimized C implementation runs in approximately 0.4 s on a 1.5-GHz Pentium 4 processor for a 1-megapixel image, and the running time is approximately proportional to the number of pixels in the image.

Finally, it can be noticed that, if the dynamic range of the input image is lower than the dynamic range  $d$  of the panels, the optimization problem admits multiple solutions, with the backpanel equal to a constant value and the front-panel proportional to the input image. This is not an issue in practice, because the different solutions produce the same visual output and can therefore be chosen arbitrarily. Moreover, in a practical implementation, the optimization problem is solved numerically by means of an iterative method, which converges to just one solution depending on the initialization. A modification in the objective function of Eq. (11), in order to guarantee a unique solution, would actually increase the algorithm complexity without introducing a practical benefit. Moreover, this issue cannot occur if the input image is encoded following the DICOM grayscale display function.<sup>16</sup> In this case, the lowest and highest digital levels of the encoded image are mapped to the black and white levels of the display, respectively, and the dynamic range of the input image therefore has a fixed value.

## 6 Results and Open Problems

As a measure of the efficacy of the algorithm, we can compute the relative error [Eq. (2)]. The value depends on the image and on the displacement  $(\Delta x, \Delta y)$  of the backpanel. For the latter, we considered all the values within the limits estimated in Section 3 and took the worst case. For the test image used in Fig. 2 and following, in the worst viewing conditions, we obtained a mean absolute value of 0.03 using the proposed method, compared to 0.1 using a simple square root. However, the visibility of artifacts in an image strongly depends on their spatial distribution and cannot be easily expressed by a mean value. Complex models have been introduced<sup>17,18</sup> but still have some limitations. An accurate evaluation of the results can only be obtained by means of observer studies, which will be performed in the future.

The algorithm described in Section 5 cannot eliminate completely the parallax effects if the input image contains sharp edges which have a greater magnitude than the dynamic range  $d$  of the panels. In this case, due to the presence of the upper bound in Eq. (9), the frontpanel alone is not able to completely reproduce the edge, and a fraction of

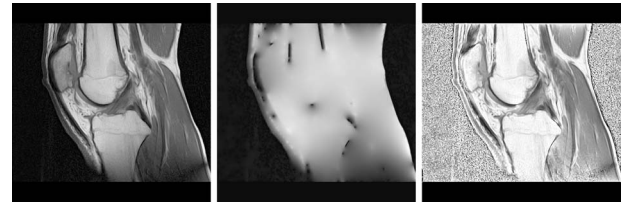


**Fig. 10** Example of splitting: (left to right) original image, backpanel, and frontpanel.

its magnitude must be transferred onto the backpanel. An edge in the backpanel becomes visible in the case of parallax error. An example is visible in Fig. 10. The source image contains sharp edges and isolated black pixels; if perfect reconstruction is requested, a very dark pixel can only be reproduced when both panels are dark, and the degrees of freedom allowed by the constraints are strongly reduced. The first proposed method does not consider an upper bound; in some cases, perfect reconstruction can be lost.

Because the upper bound was introduced to guarantee perfect reconstruction and detail preservation, we must deduce that these requirements are incompatible with that of parallax error reduction. A possible solution to this problem is to relax the perfect reconstruction constraint [Eq. (3)] and allow some distortion in the visualized image. By observing Fig. 10, it can be noticed that the dark pixels typically carry little information content; if this were true in general, one could filter the input image before the splitting in order to remove isolated black pixels and limit sharp edges. It is also known<sup>19,20</sup> that the high dynamic range of the human visual system is mainly due to local adaptation, and if a scene contains high contrast boundaries, the details near the edge appear blurred and indistinct. Because of this limitation, in some cases a reconstruction error near a sharp edge might not be visible. Research must be done to verify if this is acceptable with medical images and if it can give rise to temporal artifacts when the algorithm is applied to video sequences.

## 7 Conclusions and Further Work

In this paper we presented a prototype of a high dynamic range display based on dual-layer LCD technology. The prototype exhibits a dynamic range of over 4 orders of magnitude, surpassing the performance of conventional radiographic film and standard displays. We presented some image-processing algorithms which reduce in most cases the parallax error which is intrinsically present in the dual-layer technology, thus allowing an off-axis view where possible.

The splitting algorithms considered in this paper guarantee a perfect reconstruction of the image when the two panels are aligned and try to minimize the parallax error introduced by off-axis view. Simple techniques which perform the splitting on a pixel-by-pixel basis are not applicable; therefore, some spatial processing must be performed. Because of the limited dynamic range of the panels, the algorithm output must satisfy appropriate constraints in order to prevent any unwanted clipping. The first proposed method uses a constrained lowpass filter to compute the backpanel image. The method is a simple improvement on a heuristic



technique and is closely related to a well-known image-processing problem, but it has some issues, which are primarily due to the suboptimal nature of the constraints. The second proposed method generates the backpanel image by minimizing an appropriate functional. We derived the exact constraints which guarantee that both panels do not saturate and that the image is displayed exactly when the panels are aligned. The overall approach we propose is original, because the backpanel is not computed by filtering the input image but is generated by means of an optimization procedure.

The prototypes and the image-processing algorithms are still under development. Concerning the hardware aspect, it might be possible to increase the total brightness by using a backpanel with a lower resolution, which typically has a higher transmittance because a smaller fraction of area is occupied by the electrical wirings. This is not possible yet with the current prototypes, because the 1.3-megapixel ( $1280 \times 1024$  pixel) panels we are using have a 5:4 aspect ratio, which is not available at lower resolutions. However, we are planning to build 5-megapixel prototypes, which also have a 5:4 aspect ratio, and in this case a 5-megapixel frontpanel can be coupled with a 1.3-megapixel backpanel. This technique only aims to increase the brightness and is not likely to reduce the computational cost of the splitting algorithm, because the frontpanel must be sharpened in any case, taking care to prevent the clipping. For the same reason, it is not advisable to introduce a diffuser foil between the two layers in order to blur the backpanel. On the contrary, a diffuser would absorb some light, thus reducing the total brightness, and further increase the distance between the panels, thus increasing the parallax error. Concerning the software aspect, we are currently working on an improved algorithm which attempts to overcome the physical limitation of HDR displays described at the end of Section 3 by taking into account the limited sensitivity of the HVS. We are also planning to run some tests in cooperation with radiologists in order to verify the benefits of the dual-layer concept and the efficacy of the image-splitting algorithms on a large sample of real reference medical images and in a real operating environment. This will provide valuable feedback on the quality of the results and on the visibility of any residual artifacts. Finally, the problem of DICOM compliance<sup>16</sup> in HDR displays is under study.

### Acknowledgments

This research was partially supported by grants from the University of Trieste and the Regione Friuli-Venezia Giulia within the "Eladin" project. The authors thank Silvio Bonfiglio of FIMI-Philips for helpful discussions and encouragement throughout this work.

### References

1. H. M. Visser, J. J. W. M. Rosink, N. Raman, and R. Rajae-Joorens, "Invited paper: Tuning LCD displays to medical applications," in *Proc. Intl. Display Research Conf. (EuroDisplay 2005)*, 19–22 September 2005, Edinburgh, Scotland, pp. 74–77, SID, Campbell, CA (2005).
2. H. Seetzen, W. Heidrich, W. Stuerzlinger, G. Ward, L. A. Whitehead, M. Trentacoste, A. Gosh, and A. Vorozcovs, "High dynamic range display systems," in *Proc. ACM SIGGRAPH 2004*, HDR and perception, pp. 760–768, ACM, New York (2004).
3. M. Trentacoste, W. Heidrich, L. Whitehead, H. Seetzen, and G. Ward, "Photometric image processing for high dynamic range displays," *J. Visual Commun. Image Represent* **18**, 439–451 (2007).

4. H. Seetzen, S. Makki, H. Ip, T. Wan, V. Kwong, G. Ward, W. Heidrich, and L. Whitehead, "Self-calibrating wide color gamut high dynamic range display," *Proc. SPIE* **6492**, 64920Z (2007).
5. P. A. Penz, "Stacked electro-optic display," U.S. Patent No. 4,364,039 (1982).
6. Recommendation ITU-R BT.709-4, *Parameter Values for the HDTV Standards for Production and International Programme Exchange*, 2000.
7. E. H. Land and J. J. McCann, "Lightness and Retinex theory," *J. Opt. Soc. Am.* **61**, 1–11 (1971).
8. E. H. Land, "The Retinex theory of color vision," *Sci. Am.* **237**, 108–128 (1977).
9. J. A. Frankle and J. J. McCann, "Method and apparatus for lightness imaging," U.S. Patent No. 4,384,336 (1983).
10. J. McCann, "Lessons learned from Mondrians applied to real images and color gamuts," in *Proc. IS&T/SID Seventh Color Imaging Conference*, pp. 1–8, SID, Campbell, CA (1999).
11. D. Shaked and R. Keshet, "Robust recursive envelope operators for fast Retinex," Technical report HPL-2002-74R1, HP Laboratories Israel, March 2004.
12. R. Kimmel, M. Elad, D. Shaked, R. Keshet, and I. Sobel, "A variational framework for Retinex," *Int. J. Comput. Vis.* **52**(1), 7–23 (2003).
13. R. Kimmel, D. Shaked, M. Elad, and I. Sobel, "Space-dependent color gamut mapping: A variational approach," *IEEE Trans. Image Process.* **14**, 796–803 (2005).
14. A. Brandt, "Multi-level adaptive solutions to boundary-value problems," *Math. Comput.* **31**, 333–390 (1977).
15. W. Hackbusch, *Multigrid Methods and Applications*, Springer, Berlin (1985).
16. National Electrical Manufacturers Association, *Digital Imaging and Communications in Medicine (DICOM). Part 14: Grayscale Standard Display Function* (2007).
17. S. Daly, *The Visible Differences Predictor: An Algorithm for the Assessment of Image Fidelity*, pp. 179–206, MIT Press, Cambridge, MA (1993).
18. R. Mantiuk, K. Myszkowski, and H.-P. Seidel, "Visible difference predictor for high dynamic range images," in *Proc. IEEE International Conference on Systems, Man and Cybernetics*, pp. 2763–2769 (2004).
19. P. Moon and D. Spencer, "The visual effect of nonuniform surrounds," *J. Opt. Soc. Am.* **35**(3), 233–248 (1945).
20. J. Vos, "Disability glare—a state of the art report," *CIE J.* **3**(2), 39–53 (1984).



**Gabriele Guarnieri** obtained a degree in electronics engineering at the University of Trieste in 2005, with a score of 110/110 cum laude and a thesis on digital image processing. He is currently a PhD student in informations engineering—signal and image processing at the University of Trieste, under the supervision of Prof. Giovanni Ramponi. He was a visiting researcher at the Image Processing Research Laboratory of the University of

California, Santa Barbara, working with Prof. Sanjit Mitra, and at the Center for Devices and Radiological Health of the U.S. Food and Drug Administration in Silver Spring, MD, working with Dr. Aldo Badano. His primary research topic is the processing of high-dynamic-range images and video and includes, in addition to the development of algorithms, hardware implementation and the psychophysical evaluation of image quality. A research contract with FIMI-Philips of Saronno (VA, Italy) is also in progress and aims at the development of a novel high-dynamic-range LCD display for medical imaging applications.



**Luigi Albani** joined Philips Research in 1987, where he was involved in the development of a new high-definition TV European standard. His main research dealt image enhancement for HDTV Studio Cameras, MPEG2 Decoding, HDTV-SDTV format converters, and pre-post processing of low bit-rate coding H263 Videoconferencing system. Since 1998, he has been working on LCD monitor architectures and image enhancement ASIC design within Philips Consumer Electronics. Currently, he is leading the FIMI-Philips innovation team in working on LCD monitor development for

medical applications such as endoscopy and X-ray modalities, dealing primarily with LCD monitor architecture and processing, LED backlight technology, and high-dynamic-range displays. He is a member of the Society for Information Display and SPIE.



**Giovanni Ramponi** received a degree in electronic engineering (summa cum laude) in 1981; since 2000 he has been a professor of electronics in the Department of Electronics at the University of Trieste, Italy. His research interests include nonlinear digital-signal processing and in particular the enhancement and feature extraction in images and image sequences. Prof. Ramponi has been an associate editor of the IEEE Signal Processing Letters and of

the IEEE Transactions on Image Processing; presently he is an associate editor of the SPIE Journal of Electronic Imaging. He has participated in various European and national research projects. He is the co-inventor of various pending international patents and has published about 150 papers in international journals and conference proceedings and as book chapters. He is a senior member of the IEEE.